

Journal of Visualized Experiments

High-Resolution 3D Imaging of Rabies Virus Infection in Solvent-Cleared Brain Tissue

--Manuscript Draft--

Article Type:	Invited Methods Collection - JoVE Produced Video
Manuscript Number:	JoVE59402R2
Full Title:	High-Resolution 3D Imaging of Rabies Virus Infection in Solvent-Cleared Brain Tissue
Keywords:	Confocal laser scanning microscopy; uDISCO; iDISCO; Immunofluorescence; tissue clearing; optical clearing; deep-tissue antibody labeling; 3D imaging; rabies virus; brain; neuroinvasion; pathogenesis
Corresponding Author:	Stefan Finke Friedrich-Loeffler-Institut, Federal Research Institute of Animal Health Greifswald - Isle of Riems, Mecklenburg-West Pomerania GERMANY
Corresponding Author's Institution:	Friedrich-Loeffler-Institut, Federal Research Institute of Animal Health
Corresponding Author E-Mail:	stefan.finke@fli.de
Order of Authors:	Luca Zaeck Madlin Potratz Conrad M. Freuling Thomas Müller Stefan Finke
Additional Information:	
Question	Response
Please indicate whether this article will be Standard Access or Open Access.	Standard Access (US\$2,400)
Please indicate the city, state/province, and country where this article will be filmed . Please do not use abbreviations.	Greifswald - Isle of Riems, Mecklenburg-West Pomerania, Germany



FRIEDRICH-LOEFFLER-INSTITUT

seit 1910

FLI

Bundesforschungsinstitut für Tiergesundheit
Federal Research Institute for Animal Health



Collaborating Centre for Zoonoses in Europe

Friedrich-Loeffler-Institut | Postfach 1318 | 17466 Greifswald-Insel Riems

**Institute of Molecular Virology and
Cell Biology**

Leiter:

Prof. Dr. Dr. h.c. Thomas C.
Mettenleiter

bearbeitet von: PD Dr. Stefan Finke

Telefon: 038351 71283

Fax: 038351 71151

E-Mail: stefan.finke@fli.de

Datum: 11.01.2019

Revised Manuscript Submission to JoVE

Manuscript number: JoVE59402R1

Dear Dr. Rupprecht,
Dear Sir or Madam,

We are very thankful for the editorial comments to our manuscript. As before, we have addressed all comments in the rebuttal document and revised our manuscript accordingly.

Having done so, we hope that all scientific, content-related, and stylistic requirements are now met and that our manuscript is ready for publication in JoVE.

Sincerely,

Stefan Finke, Scientific Director

Hauptsitz - Insel Riems
Südufer 10
17493 Greifswald - Insel Riems
Telefon: +49 38351 7-0
Fax: +49 38351 7-1151
www.fli.bund.de

Standort Braunschweig
Bundesallee 50
38116 Braunschweig
Telefon: +49 531 596-3102
Fax: +49 531 596-3299
www.fli.bund.de

Standort Celle
Dörnbergstraße 25/27
29223 Celle
Telefon: +49 5141 3846-0
Fax: +49 5141 3846-117
www.fli.bund.de

Standort Jena
Naumburger Straße 96a
07743 Jena
Telefon: +49 3641 804-2100
Fax: +49 3641 804-2228
www.fli.bund.de

Standort Mariensee
Höltysstraße 10
31535 Neustadt
Telefon: +49 5034 871-0
Fax: +49 5034 871-143
www.fli.bund.de

TITLE:

High-resolution 3D Imaging of Rabies Virus Infection in Solvent-cleared Brain Tissue

AUTHORS AND AFFILIATIONS:

Luca Zaeck¹, Madlin Potratz¹, Conrad M. Freuling¹, Thomas Müller¹, Stefan Finke¹

¹Institute of Molecular Virology and Cell Biology, Friedrich-Loeffler-Institut, Federal Research Institute for Animal Health, Greifswald–Insel Riems, Germany

Corresponding author:

Stefan Finke (stefan.finke@fli.de)

E-mail addresses of co-authors:

Luca Zaeck (luca.zaeck@fli.de)

Madlin Potratz (madlin.potratz@fli.de)

Conrad M. Freuling (conrad.freuling@fli.de)

Thomas Müller (thomas.mueller@fli.de)

KEYWORDS:

Confocal laser scanning microscopy, uDISCO, iDISCO, immunofluorescence, tissue clearing, optical clearing, deep-tissue antibody labeling, 3D imaging, rabies virus, brain, neuroinvasion, pathogenesis

SUMMARY:

Novel, immunostaining-compatible tissue clearing techniques like the ultimate 3D imaging of solvent-cleared organs allow the 3D visualization of rabies virus brain infection and its complex cellular environment. Thick, antibody-labeled brain tissue slices are made optically transparent to increase imaging depth and to enable 3D analysis by confocal laser scanning microscopy.

ABSTRACT:

The visualization of infection processes in tissues and organs by immunolabeling is a key method in modern infection biology. The ability to observe and study the distribution, tropism, and abundance of pathogens inside of organ tissues provides pivotal data on disease development and progression. Using conventional microscopy methods, immunolabeling is mostly restricted to thin sections obtained from paraffin-embedded or frozen samples. However, the limited 2D image plane of these thin sections may lead to the loss of crucial information on the complex structure of an infected organ and the cellular context of the infection. Modern multicolor, immunostaining-compatible tissue clearing techniques now provide a relatively fast and inexpensive way to study high-volume 3D image stacks of virus-infected organ tissue. By exposing the tissue to organic solvents, it becomes optically transparent. This matches the sample's refractive indices and eventually leads to a significant reduction of light scattering. Thus, in combination with long free working distance objectives, large tissue sections up to 1 mm in size can be imaged by conventional confocal laser scanning microscopy (CLSM) at high resolution. Here, we describe a protocol to apply deep-tissue imaging after tissue clearing to visualize rabies

virus distribution in infected brains in order to study topics like virus pathogenesis, spread, tropism, and neuroinvasion.

INTRODUCTION:

Conventional histology techniques mostly rely on thin sections of organ tissues, which can inherently provide only 2D insights into a complex 3D environment. Although feasible in principle, 3D reconstruction from serial thin sections requires demanding technical pipelines for both slicing and subsequent *in silico* alignment of the acquired images¹. Moreover, seamless reconstruction of z-volumes after microtome slicing is critical as both mechanical and computational artifacts can remain because of suboptimal image registration caused by nonoverlapping image planes, staining variations, and physical destruction of tissue by, for instance, the microtome blade. In contrast, pure optical slicing of intact thick tissue samples allows the acquisition of overlapping image planes (oversampling) and, thereby, facilitates 3D reconstruction. This, in turn, is highly beneficial for the analysis of infection processes in complex cell populations (e.g., neuronal networks in the context of surrounding glial and immune cells). However, inherent obstacles of thick tissue sections include light scattering and limited antibody penetration into the tissue. In recent years, a variety of techniques has been developed and optimized to overcome these issues^{2–13}. Essentially, target tissues are turned optically transparent by treatment with either aqueous^{2–9} or organic solvent-based^{10–13} solutions. The introduction of 3DISCO (3D imaging of solvent-cleared organs)^{11,12} and its successor uDISCO (ultimate 3D imaging of solvent-cleared organs)¹³ provided a relatively fast, simple, and inexpensive tool with excellent clearing capabilities. The main constituents of the clearing protocol are the organic solvents *tert*-butanol (TBA), benzyl alcohol (BA), benzyl benzoate (BB), and diphenyl ether (DPE). The development and addition of iDISCO (immunolabeling-enabled 3D imaging of solvent-cleared organs)¹⁴, a compatible immunostaining protocol, constituted another advantage over existing methods and enabled the deep-tissue labeling of antigens of interest, as well as the long-term storage of immunostained samples. Thus, the combination of iDISCO¹⁴ and uDISCO¹³ allows for the high-resolution imaging of antibody-labeled proteins in large tissue sections (up to 1 mm) using conventional CLSM.

The preservation of an organ's complex structure in all three dimensions is particularly important for brain tissue. Neurons comprise a very heterogeneous cellular subpopulation with highly diverse 3D morphologies based on their neurite projections (reviewed by Masland¹⁵). Furthermore, the brain consists of a number of compartments and subcompartments, each composed of different cellular subpopulations and ratios thereof, including glial cells and neurons (reviewed by von Bartheld et al.¹⁶). As a neurotropic virus, the rabies virus (RABV, reviewed by Fooks et al.¹⁷) primarily infects neurons, using their transport machinery to travel in retrograde direction along axons from the primary site of infection to the central nervous system (CNS). The protocol described here (**Figure 1A**) allows for the immunostaining-assisted detection and visualization of RABV and RABV-infected cells in large, coherent image stacks obtained from infected brain tissue. This enables an unbiased, 3D high-resolution assessment of the infection environment. It is applicable to brain tissue from a variety of species, can be performed immediately after fixation or after the long-term storage of samples in paraformaldehyde (PFA), and allows the storage and reimaging of stained and cleared samples for months.

PROTOCOL:

RABV-infected, PFA-fixed archived brain material was used. The respective animal experimental studies were evaluated by the responsible animal care, use, and ethics committee of the State Office for Agriculture, Food Safety, and Fishery in Mecklenburg-Western Pomerania (LALFF M-V) and gained approval with permissions 7221.3-2.1-002/11 (mice) and 7221.3-1-068/16 (ferrets). General care and methods used in the animal experiments were carried out according to the approved guidelines.

CAUTION: This protocol uses various toxic and/or harmful substances, including PFA, methanol (MeOH), hydrogen peroxide (H₂O₂), sodium azide (NaN₃), TBA, BA, BB, and DPE. MeOH and TBA are highly flammable. Avoid exposure by wearing appropriate personal protective equipment (a lab coat, gloves, and eye protection) and conducting experiments in a fume hood. Collect waste separately in appropriate containers and dispose of it according to local regulations. Rabies virus is classified as a biosafety level (BSL)-2 pathogen and can, therefore, generally be handled under BSL-2 conditions. Some activities, including procedures that may generate aerosols, work with high virus concentrations, or work with novel lyssaviruses, may require BSL-3 classification. Pre-exposure prophylaxis is recommended for high-risk personnel, including animal caretakers and laboratory workers^{18,19}. Refer to local authority regulations.

1. Fixation of brain tissue and sectioning

1.1. Fix brain samples in an appropriate volume of 4% PFA in phosphate-buffered saline (PBS [pH 7.4]) for at least 48 h at 4 °C (with an approximate tissue-to-fixative ratio of 1:10 [v/v]).

1.2. Wash the tissue samples 3x in PBS for at least 30 min each wash and store them in 0.02% NaN₃/PBS at 4 °C until use.

1.3. Section the tissue into 1 mm-thick sections using a vibratome (blade feed rate: 0.3–0.5 mm/s, amplitude: 1 mm, slice thickness: 1,000 µm).

1.4. To retain the correct slice sequence, store each tissue section separately in a well of a multiwell cell culture plate. Add 0.02% NaN₃/PBS and store the tissue sections at 4 °C until use.

2. Sample pretreatment with methanol

NOTE: Perform all incubation steps with gentle oscillation and, if not indicated otherwise, at room temperature. Protect the sample from light. The sample pretreatment serves the overall purpose of improving antibody diffusion and reducing tissue autofluorescence by exposure to MeOH and H₂O₂, respectively¹⁴.

2.1. Prepare 20% (v/v), 40%, 60%, and 80% MeOH solutions in distilled water. For instance, for 20% MeOH, add 10 mL of 100% MeOH to 40 mL of distilled water in an appropriate sealable vessel and mix by inverting it.

2.2. Transfer the samples to reasonably sized vessels (e.g., 5 mL reaction tubes). Take care to use materials chemically resistant to the reagents used in this protocol. For instance, note that while polypropylene is suitable, polystyrene is not.

NOTE: The volume specifications in this protocol refer to 5 mL reaction tubes. If a different vessel is used, adjust the volumes accordingly.

2.3. Incubate the samples in 4 mL of each concentration of the prepared series of MeOH solutions in ascending order for 1 h each.

2.4. Incubate the samples 2x for 1 h each in pure (100%) MeOH.

2.5. Cool the samples to 4 °C (e.g., in a laboratory-safe refrigerator).

2.6. Prepare bleaching solution (5% H₂O₂ in MeOH) by, for instance, diluting a 30% H₂O₂ stock solution 1:6 in pure (100%) MeOH, and chill it at 4 °C.

2.7. Remove the 100% MeOH from the refrigerated samples and add 4 mL of prechilled bleaching solution (5% H₂O₂ in MeOH). Incubate overnight at 4 °C.

2.8. Exchange the bleaching solution for 4 mL of 80% MeOH and incubate for 1 h. Continue using the prepared series of MeOH solutions in descending order for 1 h each until the samples have been incubated for 1 h in 4 mL of 20% MeOH.

2.9. Wash the samples 1x for 1 h with 4 mL of PBS.

3. Immunostaining

NOTE: Perform all incubation steps with gentle oscillation and, if not indicated otherwise, at room temperature. Protect the samples from light. To prevent microbial growth, add NaN₃ to a final concentration of 0.02% to the solutions in this section. Tissue samples are further permeabilized by treatment with nonionic detergents Triton X-100 and Tween 20. Normal serum is used to block unspecific antibody binding. Glycine and heparin are added to reduce the immunolabeling background¹⁴.

3.1. Wash the samples 2x for 1 h each in 4 mL of 0.2% Triton X-100/PBS.

3.2. Permeabilize the samples for 2 days at 37 °C with 4 mL of 0.2% Triton X-100/20% DMSO/0.3 M glycine/PBS.

3.3. Block the unspecific binding of antibodies by incubating the samples for 2 days at 37 °C in 4 mL of 0.2% Triton X-100/10% DMSO/6% normal serum/PBS.

NOTE: Use normal serum from the same species the secondary antibody was raised in to achieve ideal blocking results.

3.4. Incubate the samples in 2 mL of primary antibody solution (3% normal serum/5% DMSO/PTwH [PBS-Tween 20 with heparin] + primary antibody/antibodies) for 5 days at 37 °C. Refresh the primary antibody solution 1x after 2.5 days.

3.4.1. For PTwH, reconstitute the heparin sodium salt in distilled water to make a 10 mg/mL stock solution (store this solution, aliquoted, at 4 °C). Add the stock solution to 0.2% Tween 20/PBS to a final concentration of 10 µg/mL.

NOTE: Choosing the correct antibody dilution may require optimization. Generally, standard immunohistochemistry concentrations are a good starting point.

3.5. Wash the samples for 1 day in 4 mL of PTwH, exchanging the wash buffer at least 4x–5x during the course of the day and leaving the final wash on overnight.

3.6. Incubate the samples in 2 mL of secondary antibody solution (3% normal serum/PTwH + secondary antibody/antibodies) for 5 days at 37 °C. Refresh the secondary antibody solution 1x after 2.5 days.

3.6.1. Dilute the secondary antibody/antibodies at 1:500 in secondary antibody solution (i.e., 4 µL in 2 mL).

3.7. Wash the samples for 1 day as described in step 3.5, leaving the final wash on overnight.

4. Nuclear staining

NOTE: Perform all incubation steps with gentle oscillation and, if not indicated otherwise, at room temperature. Protect the samples from light. If no nuclear staining is required or the excitation wavelength/emission spectrum of TO-PRO-3 is required for the excitation or detection of another fluorophore, skip this step.

4.1. Dilute the nucleic acid stain TO-PRO-3 at 1:1,000 in PTwH and incubate the samples in 4 mL of nuclear staining solution for 5 h.

4.2. Wash the samples for 1 day as described in step 3.5, leaving the final wash on overnight.

NOTE: Following the washes, the samples can be stored in PBS at 4 °C until optical clearing.

5. Tissue clearing

NOTE: Perform all incubation steps with gentle oscillation and, if not indicated otherwise, at room temperature. Protect the samples from light. The tissue samples are dehydrated in a graded

series of TBA solutions. As immunostaining requires aqueous solutions, all staining procedures have to be finished prior to tissue clearing. Optical clearance and refractive index matching are achieved by treatment with a mixture of BA, BB, and DPE. The clearing solution is supplemented with DL- α -tocopherol as an antioxidant¹³.

5.1. Prepare 30% (v/v), 50%, 70%, 80%, 90%, and 96% TBA solutions in distilled water. For instance, for 30% TBA, add 15 mL of 100% TBA to 35 mL of distilled water in an appropriate sealable vessel and mix by inverting.

NOTE: TBA has a melting point of 25–26 °C; thus, it tends to be solid at room temperature. In order to prepare TBA solutions, heat the well-sealed bottle at 37 °C in an incubator or water bath.

5.2. Dehydrate the samples with 4 mL of each concentration of the prepared series of TBA solutions in ascending order for 2 h each. Leave the 96% TBA on overnight.

5.3. Dehydrate the samples further in pure (100%) TBA for 2 h.

5.4. Prepare clearing solution BABB-D15.

NOTE: BABB-D15 is a combination of BA and BB (BABB) which is mixed with DPE at a ratio of x:1, where x is specified in the solution's name, in this case 15.

5.4.1. For BABB, mix one-part BA with two parts BB.

5.4.2. Mix BABB and DPE at a ratio of 15:1.

5.4.3. Add 0.4 vol% DL- α -tocopherol (vitamin E).

NOTE: For example, for 20 mL of BABB-D15, mix 6.25 mL of BA with 12.5 mL of BB. Add 1.25 mL of DPE and supplement it with 0.08 mL of DL- α -tocopherol.

5.5. Clear the samples in clearing solution until they are optically transparent (2–6 h).

5.6. The samples can be stored at 4 °C in BABB-D15, protected from light, until mounting and imaging.

6. Sample mounting

6.1. Using a 3D printer, print an imaging chamber and lid (material: copolyester [CPE], nozzle: 0.25 mm, layer height: 0.06 mm, wall thickness: 0.88 mm, wall count: 4, infill: 100%, no support structure; the corresponding .STL file can be found in the **Supplementary Materials** of this protocol).

6.2. Assemble the imaging chamber (**Figure 2**).

6.2.1. Mount a round coverslip (diameter: 30 mm) on the imaging chamber with RTV-1 (one-component room-temperature-vulcanizing) silicone rubber. Remove the excess silicone rubber and cure overnight.

6.2.2. Mount a round coverslip (diameter: 22 mm) on the lid with RTV-1 silicone rubber. Remove any excess silicone rubber and cure overnight.

6.3. Place the sample in an imaging chamber, add a small volume of BABB-D15, and insert the lid. Fill the chamber up with BABB-D15 through the inlet, using a hypodermic needle (27 G x 3/4 inch [0.40 mm x 20 mm]).

6.4. Plug the inlet and seal the imaging chamber with RTV-1 silicone rubber. Cure overnight in the dark.

7. Imaging and image processing

7.1. Set up the image acquisition by selecting the respective laser lines to match the fluorophores used. Adjust the detection ranges of each detector to prevent signal overlap between channels.

NOTE: Exemplary detection ranges for Alexa Fluor 488, Alexa Fluor 568, and TO-PRO-3 are 500–550 nm, 590–620 nm, and 645–700 nm, respectively.

7.2. Choose the acquisition parameters, define the upper and lower border of the z-stack, and acquire the image stack.

NOTE: Exemplary acquisition parameters are a sequential scan with a pixel size of 60–90 nm, a z-step size of 0.5 μm , a line average of 1, a scan speed of 400 Hz, and a pinhole size of 1 Airy unit.

7.3. Process the image stack using appropriate image analysis software (e.g., Fiji) to generate 3D projections or perform in-depth analyses.

NOTE: Because of the large size of the acquired image files, the use of a workstation is usually necessary.

7.3.1. Open the acquisition or image file(s) in Fiji (**File | Open | Select files**).

7.3.1.1. If using, for instance, .LIF files, select or deselect the desired options in the Bio-Formats dialog window. View stack with **Hyperstack**. Other than that, no specific selections or ticks are necessary. Press **OK**.

7.3.1.2. If the file contains multiple image stacks, select the ones to be analyzed and confirm by pressing **OK**.

7.3.2. Perform bleach correction by splitting the merged image into individual channels (**Image | Color | Channels Tool**, then select **More | Split Channels**). For each channel, select **bleach correction** (**Image | Adjust | Bleach Correction**) and choose **Simple Ratio** (background intensity: 0.0).

NOTE: In some cases, for instance, when there is no linear decay of the signal or the signal is too weak overall, **Simple Ratio** may fail. Alternatively, try **Exponential Fit** or skip the bleach correction.

7.3.3. Adjust the brightness and contrast for each channel using the sliders (**Image | Adjust | Brightness | Contrast**).

7.3.4. Merge the channels (**Image | Color | Merge Channels**), make a composite (**Image | Color | Channels Tool**, then select **More | Make Composite**), and convert it to RGB format (**Image | Color | Channels Tool**, then select **More | Convert to RGB**).

7.3.5. If necessary, resize the image stack to reduce the computation time and file size (**Image | Adjust | Size**, both options ticked plus bilinear interpolation).

7.3.6. Generate a 3D projection (**Image | Stacks | 3D Project**). Choose **Brightest Point** as projection method and set the slice spacing to match the z-step size of the acquired image stack. For maximum quality, set the rotation angle increment to **1** and enable interpolation. Modify the total rotation, transparency thresholds, and opacity as needed.

7.3.7. If necessary, readjust the contrast and brightness by converting the 3D projection back to 8-bit format (**Image | Type | 8-bit**). Use the respective sliders (**Image | Adjust | Brightness | Contrast**) and reconvert the image stack to RGB format as described in step 7.3.4.

7.3.8. Save the 3D projection as .TIF file (image file format) and .AVI file (video file format).

REPRESENTATIVE RESULTS:

The combination of iDISCO¹⁴ and uDISCO¹³ coupled with high-resolution CLSM provides deep insights into the spatiotemporal resolution and plasticity of RABV infection of brain tissue and the surrounding cellular context.

Using immunostaining of RABV phosphoprotein (P), complex layers of infected neuronal cells can be visualized in thick sections of mouse brains (**Figure 3**). Subsequently, seamless 3D projections of the acquired image stacks can be reconstructed (**Figure 3A,B**, right panel; **Animated Figure 1**). Care has to be taken when using primary antibodies from and secondary antibodies against the species the organ material originates from. The use of anti-mouse IgG antibodies on mouse brain tissue resulted in a distinct staining of the vascular system (**Figure 3B**, left panel). Because of the high resolution the image stacks are acquired with, infection can be assessed up to a single-cell level (**Figure 4**), allowing assertions on, for instance, the abundance and distribution of antigen within the cell (**Figure 4C**).

Aside from mouse brain tissue, the protocol can also be applied to brain tissue from other animal species (e.g., ferrets) (**Figure 5; Animated Figure 2**). Sections taken from different compartments of an infected ferret brain revealed a varying degree of RABV infection (**Figure 5A–D**).

As the brain comprises many different cellular subpopulations, differentiation between these populations is vital. Using antibodies directed against cell markers, assessment of the cellular identity of infected and neighboring cells is possible. For instance, astrocytes can be differentiated via the expression of glial fibrillary acidic protein (GFAP) (**Figure 6A,C; Animated Figure 3**), while neurites can be specifically stained for microtubule-associated protein 2 (MAP2) (**Figure 6B,D; Animated Figure 4**). Simultaneously, viral proteins, in this case, RABV nucleoprotein (N), can be costained to assess the relation between infected cells and the highlighted cellular subpopulation.

FIGURE AND TABLE LEGENDS:

Figure 1: Basic principle and workflow of the protocol. (A) Graphical representation of the workflow based on the protocols from Renier et al.¹⁴ and Pan et al.¹³. (B) Two exemplary ferret brain slices, one before (left panel) and one after treatment with organic solvents (right panel). Clearing turns the tissue optically transparent as observable by the then readable text. The cleared brain slice is embedded in a 3D-printed imaging chamber (right panel).

Figure 2: Technical illustration of the 3D-printed imaging chamber. (A) Exploded view drawing of the imaging chamber. The dot-dashed lines highlight components that have to be mounted on each other using RTV-1 silicone rubber. The dashed lines represent instructions for the subsequent assembly of the chamber. (B) CAD (computer-aided design) file of the imaging chamber. The corresponding .STL file to print the imaging chamber can be found in the **Supplementary Materials**. (C) Fully assembled imaging chamber.

Figure 3: Deep-tissue imaging of RABV-infected mouse brain tissue. (A and B) Mice were infected with a recombinant vulpine street virus. RABV P staining (green) revealed infected neuronal layers with large, entangled neurite projections inside the cleared brain tissue. Nuclei were counterstained with TO-PRO-3 (blue). (B) The use of fluorophore-labeled anti-mouse IgG secondary antibodies (red) on mouse tissue resulted in a distinct labeling of the vascular system. The 3D reconstruction of the acquired image stacks enables observation from different viewing angles (A and B, right panels). The scale bars = 60 μm .

Figure 4: High-resolution image acquisition enables complex assessments up to a single-cell level. The brain was dissected from an SAD L16-infected mouse. (A) RABV P staining (green) highlights an individually infected neuron. (B and C) Detail images and projections demonstrate that in-depth analyses of antigen abundance, distribution, and localization can be performed. Nuclei were counterstained with TO-PRO-3 (blue). The scale bars = 20 μm (in panel A) and 5 μm (in panel C).

Figure 5: Deep-tissue imaging of RABV-infected ferret brain tissue. Ferrets were infected with canine street RABV. (A–D) Slices from specified areas of the brain were taken, immunostained for RABV P (green), and optically cleared. Projections demonstrate that the infected cells in different parts of the brain differ in amount and morphology. Furthermore, they highlight the applicability of the protocol to tissues other than mouse-derived. Nuclei were counterstained with TO-PRO-3 (blue). The scale bars = 60 μ m.

Figure 6: Multicolor immunofluorescence allows the costaining of cellular markers. Brain tissue slices from ferrets infected with canine street RABV were used and coimmunostained for RABV N (red) and either (A and C) GFAP (green) or (B and D) MAP2 (green). Whereas GFAP is an astrocyte marker, MAP2 specifically highlights neurites. Nuclei were counterstained with TO-PRO-3 (blue). (C and D) At the bottom, single slice extractions of the enumerated detail views from the merged projections are depicted. The scale bars = 15 μ m (in panels A and B, merge image) and 10 μ m (in panels C and D, single slice extractions).

Animated Figure 1: 3D reconstructions and detail projections of image stacks from RABV-infected mouse brains. The projections were generated from the image stacks described in Figure 3. (A and C) Representations of animations of the entire respective z-stacks. (B) A detailed projection of a 3D reconstruction of a part of the z-stack of the areas highlighted at the beginning of the video. (D) A detailed projection of a tomogram of a part of the z-stack of the areas highlighted at the beginning of the video. Green = RABV P; red = mouse IgG; blue = nuclei.

Animated Figure 2: 3D reconstructions of image stacks acquired from an RABV-infected ferret brain. The projections were generated from the image stacks described in Figure 5. (A–D) The annotations refer to the same figure and describe the respective areas of the brain the slices were taken from. Green = RABV P; blue = nuclei.

Animated Figure 3: Gradual projection of the different channels of a 3D reconstruction of an RABV-infected ferret brain costained with astrocyte marker GFAP. Projections were generated from the image stack described in Figure 6A. The gradual addition of channels starts with RABV N (red), after which follow cell nuclei (blue) and, finally, GFAP (green), while the subtraction first removes RABV N, then the cell nuclei, and eventually GFAP.

Animated Figure 4: Gradual projection of the different channels of a 3D reconstruction of an RABV-infected ferret brain costained with neuronal marker MAP2. Projections were generated from the image stack described in Figure 6B. The gradual addition of channels starts with RABV N (red), after which follow cell nuclei (blue) and, finally, MAP2 (green), while the subtraction first removes RABV N, then the cell nuclei, and eventually MAP2.

DISCUSSION:

The resurgence and further development of tissue clearing techniques in recent years^{2–14} have opened up many new possibilities to obtain high-volume image stacks of organ tissue. This provided an unparalleled and powerful tool to study, among many other topics, virus infection. The subsequent 3D reconstruction of these image stacks enables sophisticated assertions on, for

instance, virus tropism, abundance, and the time course of infection. This protocol describes the immunolabeling-assisted visualization of RABV infection in solvent-cleared brain tissue.

There are several critical steps in the preparation and acquisition of the image stacks of immunolabeled, solvent-cleared tissue. Prolonged exposure to PFA can mask epitopes and, thus, result in decreased antigenicity^{20–22}. It is, therefore, important to limit the fixation times to the necessary minimum and transfer the samples to an appropriate solution (e.g., PBS supplemented with 0.02% NaN₃ for long-term storage). However, all representative images and projections provided here have been acquired from archived brain samples, some of which had been stored in PFA for weeks, highlighting the applicability of the technique to organ material that has been exposed to PFA for extended periods of time. Similar results have been shown for human brain samples¹³. Another, if not the most, critical step is the antibody incubation. Antibody concentrations have to be chosen carefully. While in most cases, standard IHC concentrations are a good starting point for deep-tissue antibody labeling, some antigens may require additional optimization of the antibody concentration. This protocol demonstrates that both RABV N and P are readily detectable by the used antibodies. While MeOH pretreatment usually improves immunolabeling, some antigens are incompatible with this treatment. For those, Renier and colleagues¹⁴ provided an alternative MeOH-free sample pretreatment. Analysis of the acquired image stacks requires adequate computational power. Because of the large file sizes of up to several gigabytes per stack, powerful computers are needed to process the images. Postprocessing often includes the subtraction of background noise and a bleach correction to compensate for acquisition-associated bleaching effects. When measuring distances, it has to be kept in mind that, as a side effect, the tissue is shrinking during the clearing process.

In comparison to other microscopy platforms, like light sheet fluorescence microscopy (LSFM) or two-photon laser scanning microscopy (2PLSM), CLSM has the most limited working distance. Therefore, it is necessary to preslice organs to 1 mm in thickness for imaging. Additionally, CLSM has the slowest acquisition speed because of its high imaging resolution. The use of a light sheet microscope would allow for faster imaging of larger volumes up to whole-brain imaging, while simultaneously sacrificing image resolution. Another limitation is the inherent increase of tissue autofluorescence with decreasing wavelength. This renders the use of fluorophores and dyes excited by the laser line at 405 nm, including Hoechst dyes, impractical to impossible.

With respect to other tissue clearing techniques, the hybrid of iDISCO¹⁴ and uDISCO¹³ combines the most positive attributes: it is highly compatible with immunostaining, highly versatile, comparatively fast, and inexpensive, it has excellent clearing capabilities, and it is feasible with a standard confocal microscope. Moreover, this protocol is not restricted to the immunostaining and clearing of brain tissue but can also be applied to a variety of other soft tissues and pathogens, both neuroinvasive and non-neuroinvasive. In conclusion, the protocol described here represents a pipeline for high-resolution 3D imaging of RABV-infected brain tissue. The 3D reconstructions of infected brain tissue can be used to answer a variety of questions concerning RABV disease progression, pathogenesis, and neuroinvasion.

ACKNOWLEDGMENTS:

The authors thank Thomas C. Mettenleiter and Verena te Kamp for critically reading the manuscript. This work was supported by the Federal Excellence Initiative of Mecklenburg Western Pomerania and the European Social Fund (ESF) Grant KolInfekt (ESF/14-BM-A55-0002/16) and an intramural collaborative research grant on Lyssaviruses at the Friedrich-Loeffler-Institute (Ri-0372).

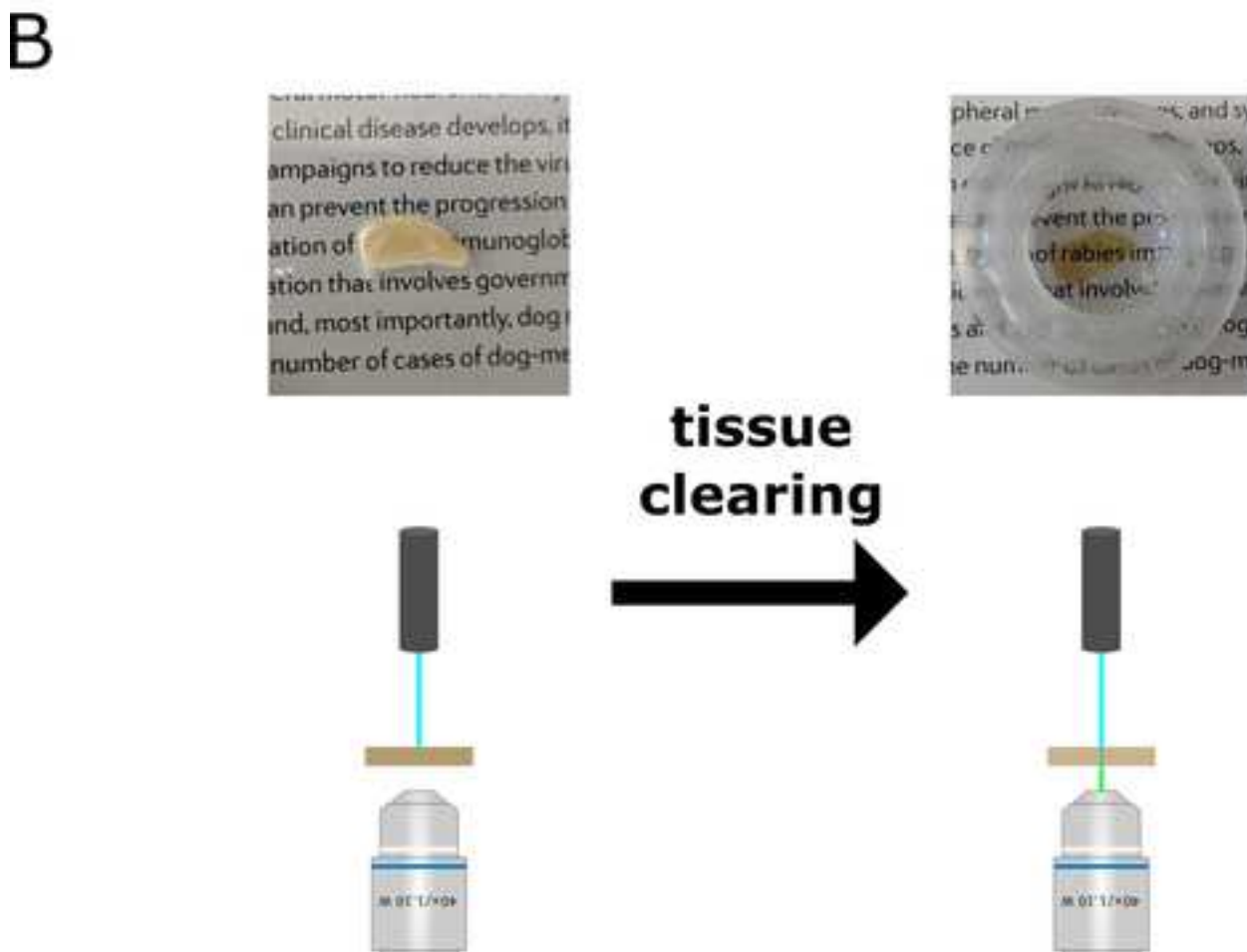
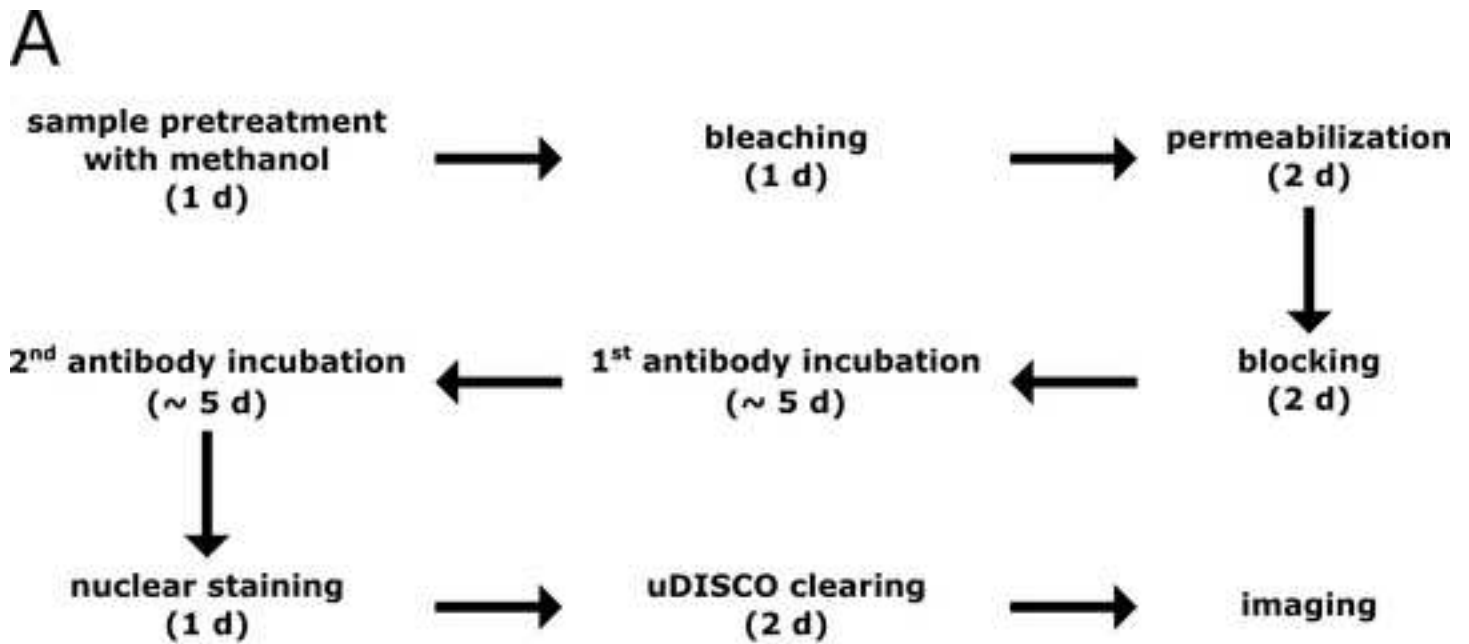
DISCLOSURES:

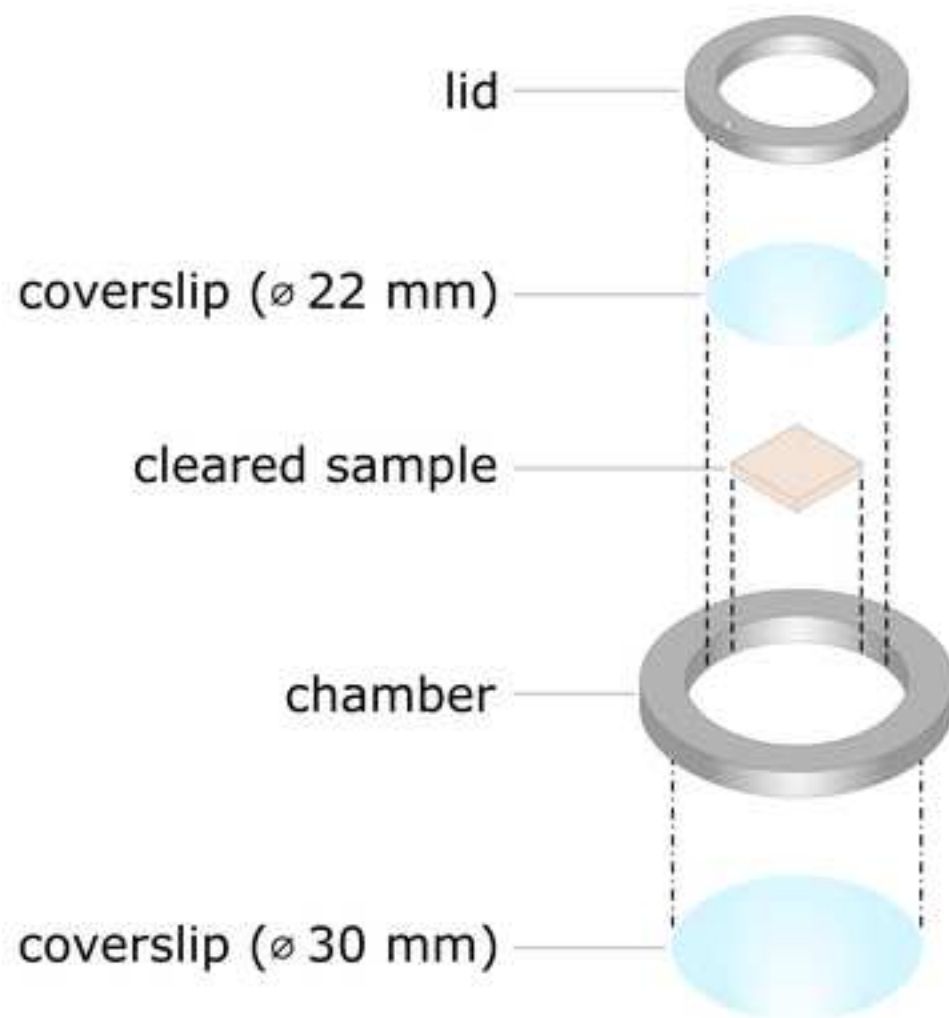
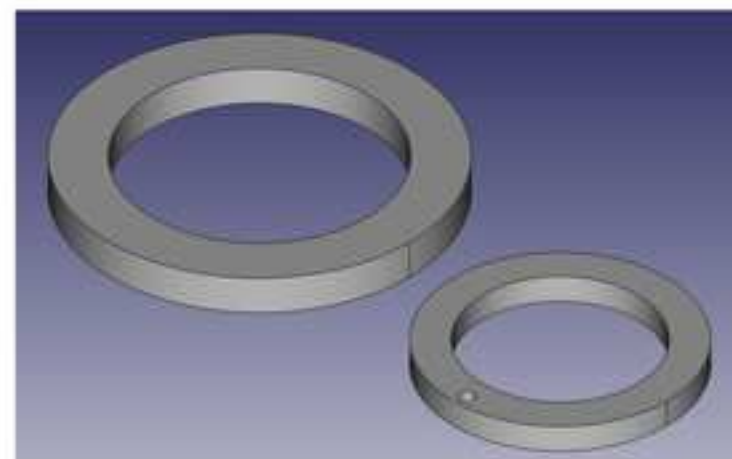
The authors have nothing to disclose.

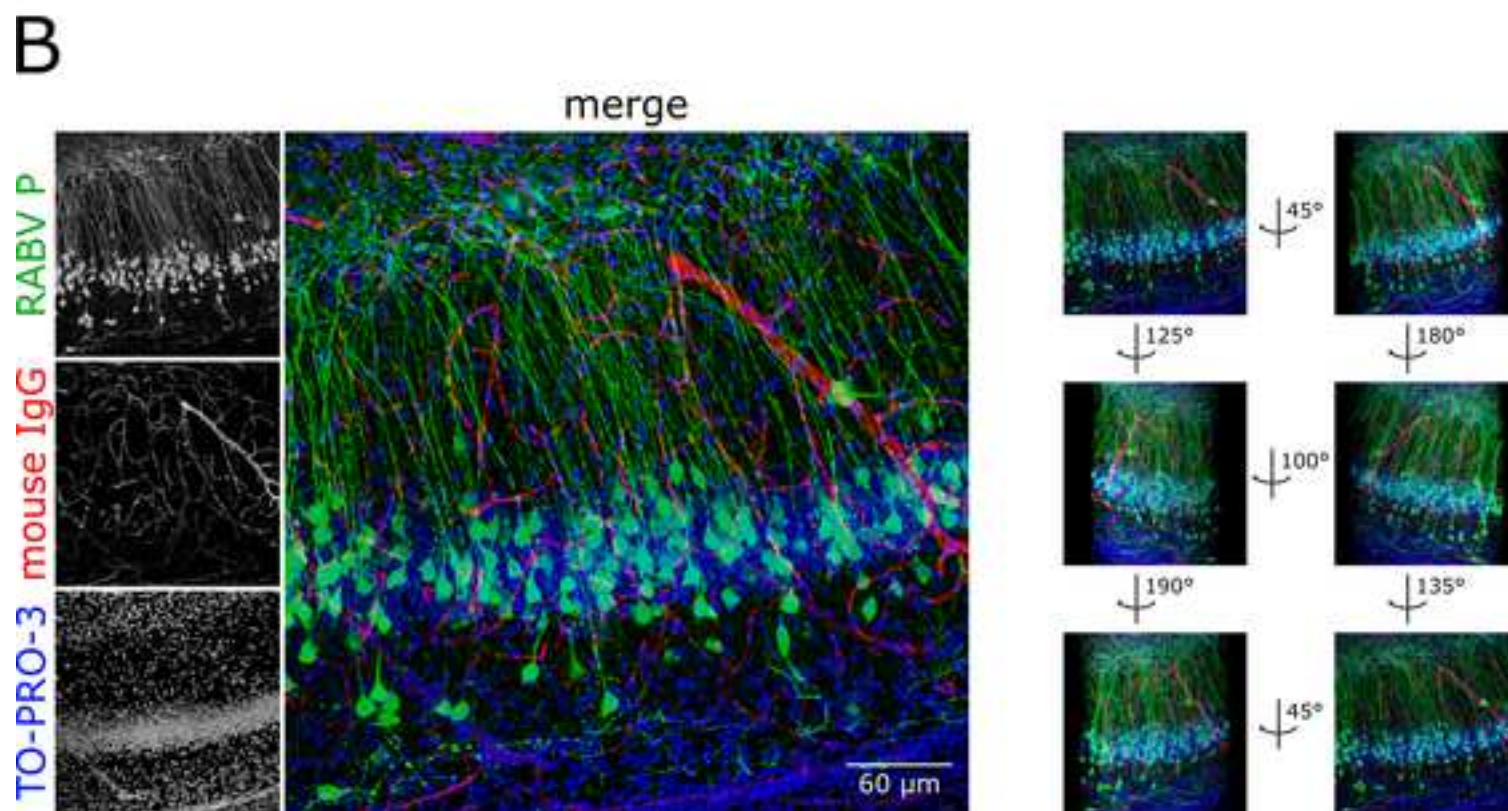
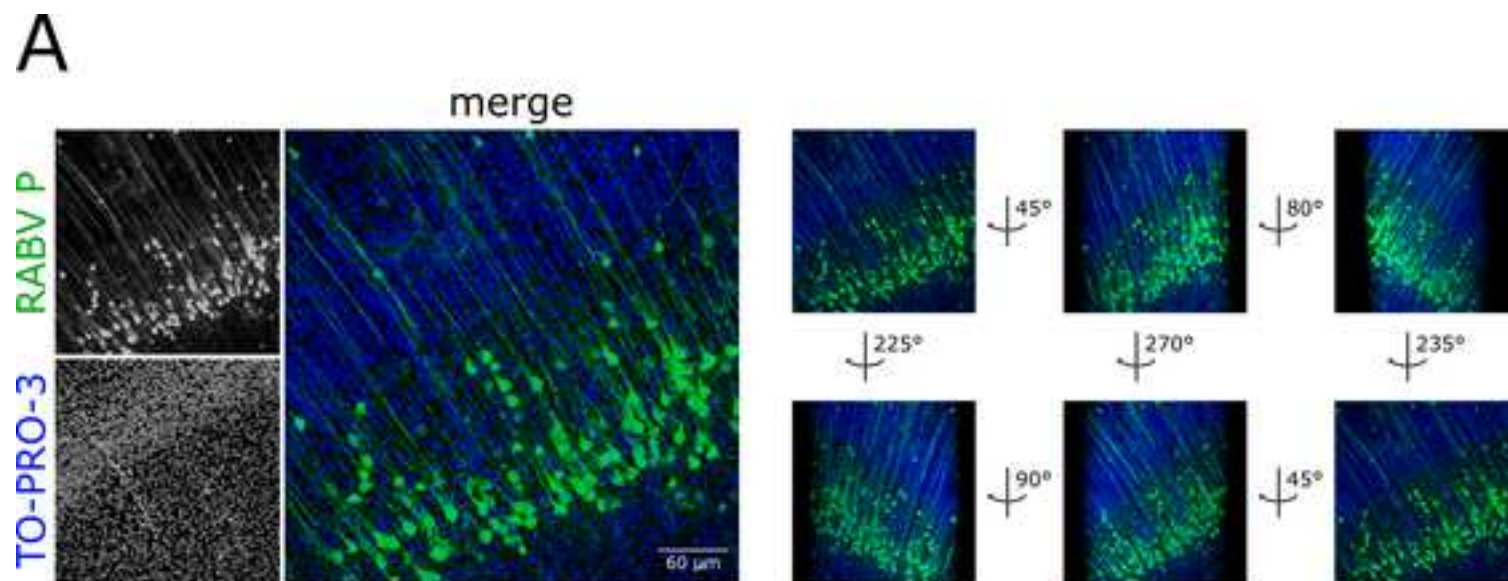
REFERENCES:

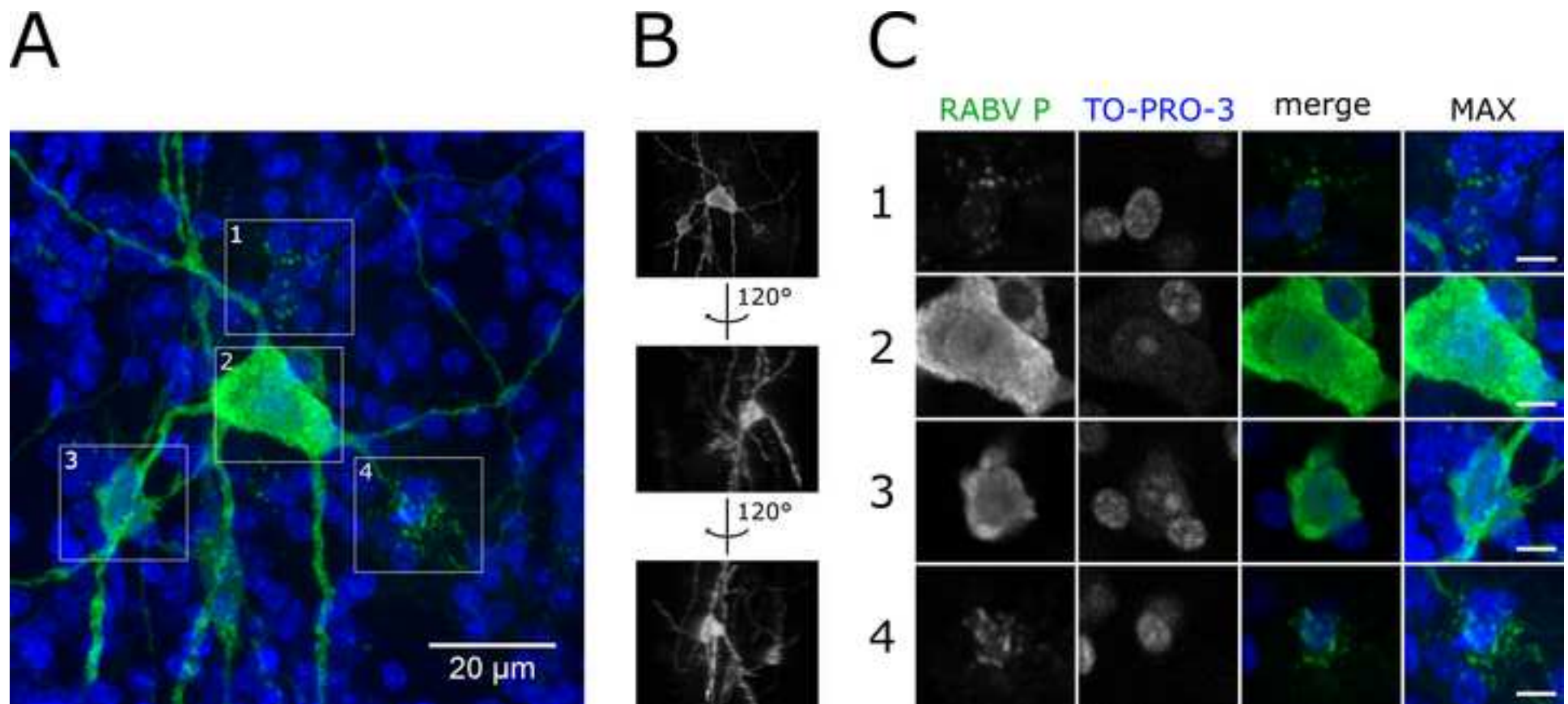
1. Pichat, J., Iglesias, J. E., Yousry, T., Ourselin, S., Modat, M. A Survey of Methods for 3D Histology Reconstruction. *Medical Image Analysis*. **46**, 73-105 (2018).
2. Chung, K. et al. Structural and molecular interrogation of intact biological systems. *Nature*. **497** (7449), 332-337 (2013).
3. Hama, H. et al. ScaleS: an optical clearing palette for biological imaging. *Nature Neuroscience*. **18** (10), 1518-1529 (2015).
4. Ke, M. T., Fujimoto, S., Imai, T. SeeDB: a simple and morphology-preserving optical clearing agent for neuronal circuit reconstruction. *Nature Neuroscience*. **16** (8), 1154-1161 (2013).
5. Kuwajima, T. et al. ClearT: a detergent- and solvent-free clearing method for neuronal and non-neuronal tissue. *Development*. **140** (6), 1364-1368 (2013).
6. Susaki, E. A. et al. Whole-brain imaging with single-cell resolution using chemical cocktails and computational analysis. *Cell*. **157** (3), 726-739 (2014).
7. Susaki, E. A. et al. Advanced CUBIC protocols for whole-brain and whole-body clearing and imaging. *Nature Protocols*. **10** (11), 1709-1727 (2015).
8. Yang, B. et al. Single-cell phenotyping within transparent intact tissue through whole-body clearing. *Cell*. **158** (4), 945-958 (2014).
9. Treweek, J. B. et al. Whole-body tissue stabilization and selective extractions via tissue-hydrogel hybrids for high-resolution intact circuit mapping and phenotyping. *Nature Protocols*. **10** (11), 1860-1896 (2015).
10. Dodt, H. U. et al. Ultramicroscopy: three-dimensional visualization of neuronal networks in the whole mouse brain. *Nature Methods*. **4** (4), 331-336 (2007).
11. Erturk, A. et al. Three-dimensional imaging of the unsectioned adult spinal cord to assess axon regeneration and glial responses after injury. *Nature Medicine*. **18** (1), 166-171 (2011).
12. Erturk, A. et al. Three-dimensional imaging of solvent-cleared organs using 3DISCO. *Nature Protocols*. **7** (11), 1983-1995 (2012).
13. Pan, C. et al. Shrinkage-mediated imaging of entire organs and organisms using uDISCO. *Nature Methods*. **13** (10), 859-867 (2016).
14. Renier, N. et al. iDISCO: a simple, rapid method to immunolabel large tissue samples for volume imaging. *Cell*. **159** (4), 896-910 (2014).
15. Masland, R. H. Neuronal cell types. *Current Biology*. **14** (13), R497-500 (2004).
16. von Bartheld, C. S., Bahney, J.,erculano-Houzel, S. The search for true numbers of neurons and glial cells in the human brain: A review of 150 years of cell counting. *The Journal of Comparative Neurology*. **524** (18), 3865-3895 (2016).
17. Fooks, A. R. et al. Rabies. *Nature Reviews Disease Primers*. **3**, 17091 (2017).

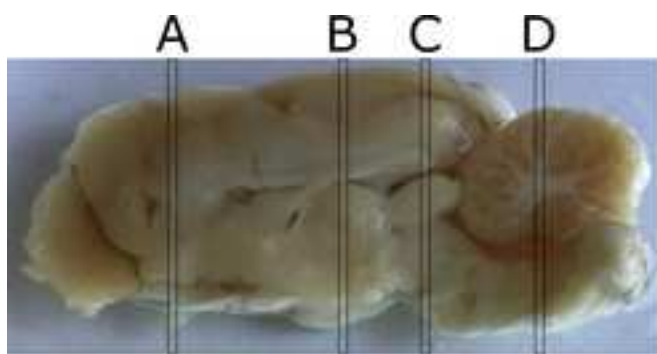
- 529 18. WHO. *WHO Expert Consultation on Rabies, Third Report. WHO Technical Report Series, No.*
530 *1012* (2018).
- 531 19. CDC. *Biosafety in Microbiological and Biomedical Laboratories, 5th Edition. US Department of*
532 *Health and Human Services* (2009).
- 533 20. Arnold, M. M. et al. Effects of fixation and tissue processing on immunohistochemical
534 demonstration of specific antigens. *Biotechnic & Histochemistry*. **71** (5), 224-230 (1996).
- 535 21. Webster, J. D., Miller, M. A., Dusold, D., Ramos-Vara, J. Effects of prolonged formalin fixation
536 on diagnostic immunohistochemistry in domestic animals. *Journal of Histochemistry and*
537 *Cytochemistry*. **57** (8), 753-761 (2009).
- 538 22. Werner, M., Chott, A., Fabiano, A., Battifora, H. Effect of formalin tissue fixation and
539 processing on immunohistochemistry. *The American Journal of Surgical Pathology*. **24** (7), 1016-
540 1019 (2000).
- 541 23. Orbanz, J., Finke, S. Generation of recombinant European bat lyssavirus type 1 and inter-
542 genotypic compatibility of lyssavirus genotype 1 and 5 antigenome promoters. *Archives of*
543 *Virology*. **155** (10), 1631-1641 (2010).
- 544



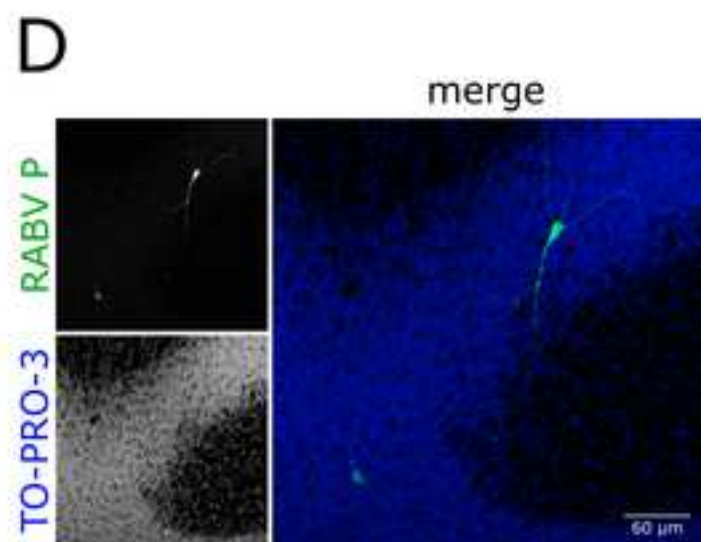
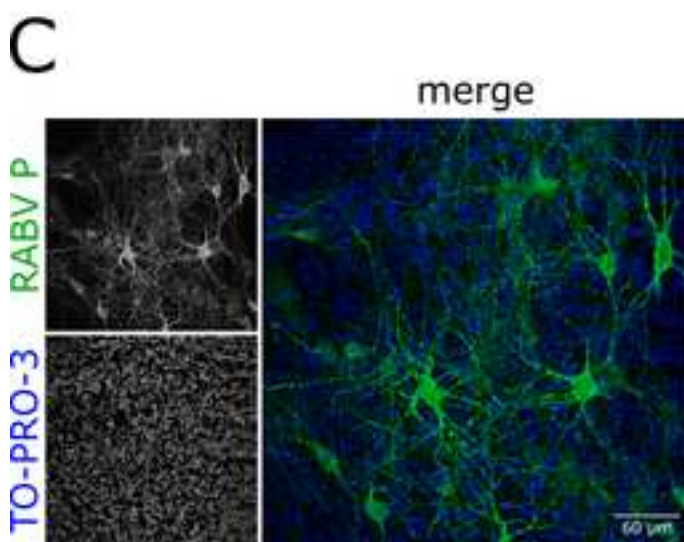
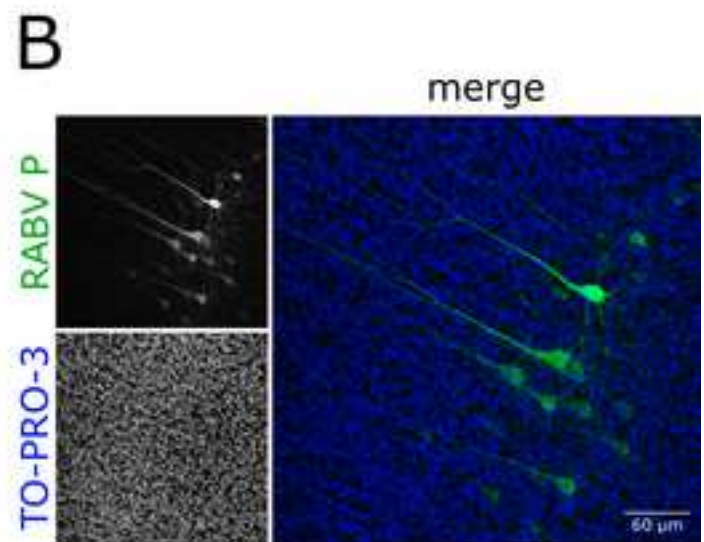
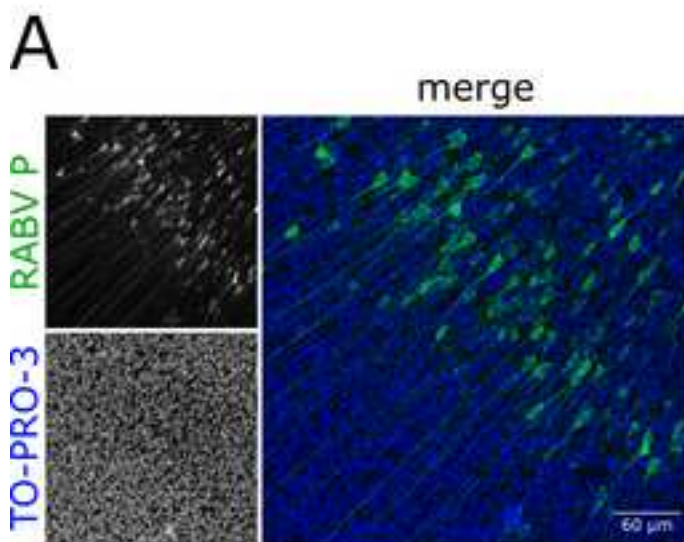
A**B****C**



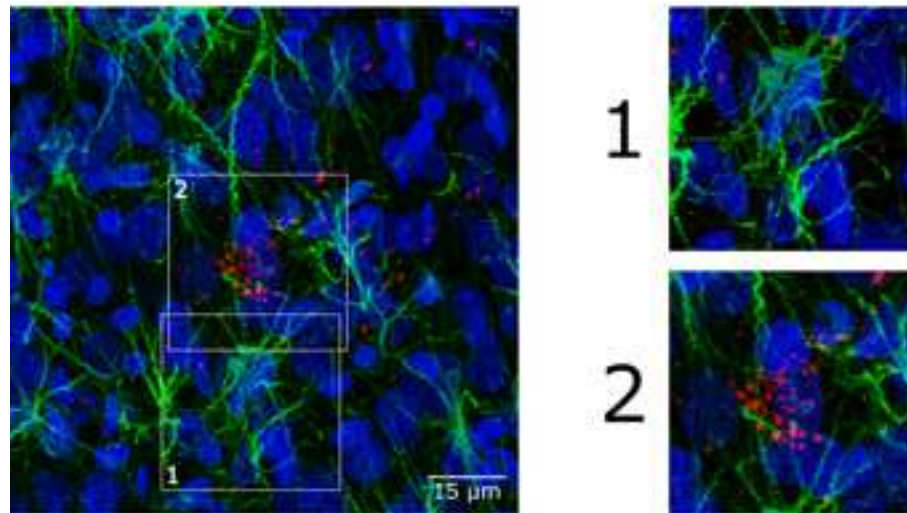




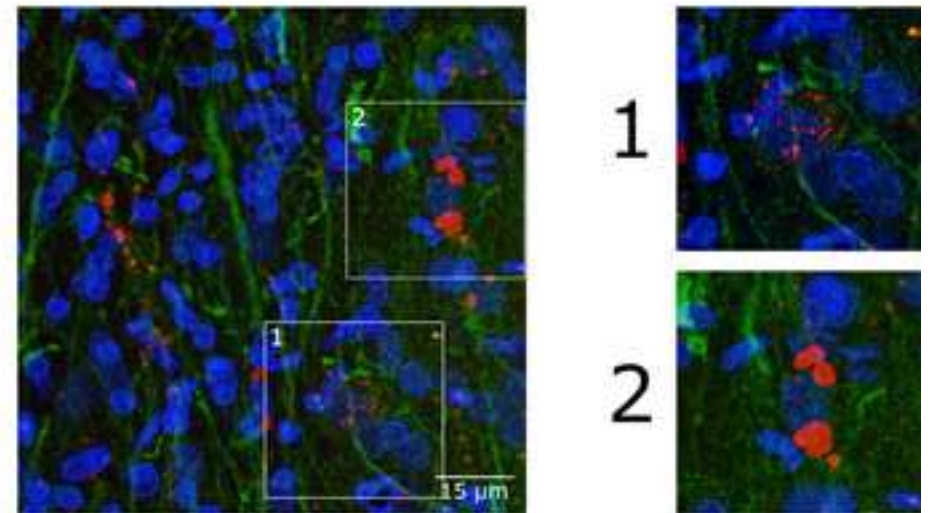
- A: Frontal lobe (gyrus, cerebral cortex, claustrum, olfactory stria)
 B: Mid-Diencephalon (subthalamus, tuber cinerium)
 C: Midbrain-Pons juncture (cadal colliculus, ventral pons)
 D: Metencephalon (cerebellum, pons)



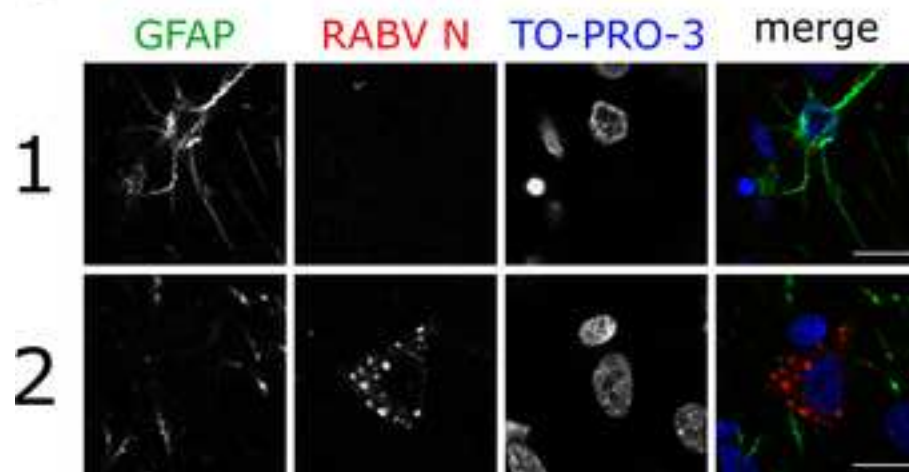
A



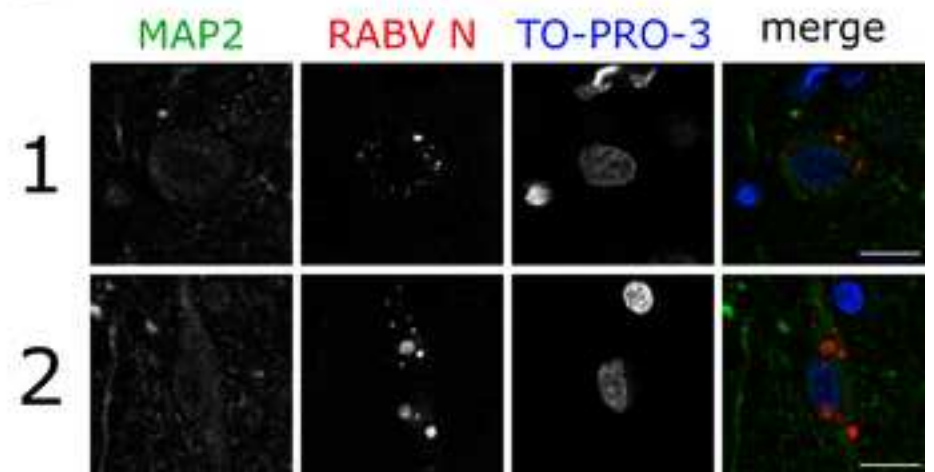
B



C



D





Click here to access/download

Video or Animated Figure

Animation1_NeuronsCombinedAnimation_compressed_r
emuxed.mp4



Click here to access/download

Video or Animated Figure

Animation2_CombinedAnimationFerretBrain_compressed_remuxed.mp4





Click here to access/download

Video or Animated Figure

Animation3_GradualChannelProjectionGFAP_compressed_remuxed.mp4





Click here to access/download

Video or Animated Figure

Animation4_GradualChannelProjectionMAP2_compressed_remuxed.mp4



Name of Material/ Equipment	Company	Catalog Number	Comments/Description
Reagents			
Benzyl alcohol	Alfa Aesar	41218	Clearing reagent
Benzyl benzoate	Sigma-Aldrich	BB6630-500ML	Clearing reagent
Dimethyl sulfoxide	Carl Roth	4720.2	Various buffers
Diphenyl ether	Sigma-Aldrich	240834-100G	Clearing reagent
DL- α -Tocopherol	Alfa Aesar	A17039	Antioxidant
Donkey serum	Bio-Rad	C06SBZ	Blocking reagent
Glycine	Carl Roth	3908.2	Background reduction
Goat serum	Merck	S26-100ML	Blocking reagent
Heparin sodium salt	Carl Roth	7692.1	Background reduction
Hydrogen peroxide solution (30 %)	Carl Roth	8070.2	Sample bleaching
Methanol	Carl Roth	4627.4	Sample pretreatment
Paraformaldehyde	Carl Roth	0335.3	Crystalline powder to make fixative solution
Sodium azide	Carl Roth	K305.1	Prevention of microbial growth in stock solutions
<i>tert</i> -Butanol	Alfa Aesar	33278	Sample dehydration for tissue clearing
TO-PRO-3	Thermo Fisher	T3605	Nucleic acid stain
Triton X-100	Carl Roth	3051.2	Detergent
Tween 20	AppliChem	A4974,0500	Detergent
Miscellaneous			
5 mL reaction tubes	Eppendorf	0030119401	Sample tubes
Coverslip, circular (diameter: 22 mm)	Marienfeld	0111620	Part of imaging chamber
Coverslip, circular (diameter: 30 mm)	Marienfeld	0111700	Part of imaging chamber
Hypodermic needle (27 G x $\frac{3}{4}$ " [0.40 mm x 20 mm])	B. Braun	4657705	Filling of the imaging chamber with clearing solution
RTV-1 silicone rubber	Wacker	Elastosil E43	Adhesive for the assembly of the imaging chamber
Ultimaker CPE 2.85 mm transparent	Ultimaker	8718836374869	Copolyester filament for 3D printer to print parts of the imaging chamber
Technical equipment and software			
3D printer	Ultimaker	Ultimaker 2+	Printing of imaging chamber
Automated water immersion system	Leica	15640019	Software-controlled water pump

Benchtop orbital shaker	Elmi	DOS-20M	Sample incubation at room temperature (~ 150 rpm)
Benchtop orbital shaker, heated	New Brunswick Scientific	G24 Environmental Shaker	Sample incubation at 37 °C (~ 150 rpm)
Confocal laser scanning microscope	Leica	DMI 6000 TCS SP5	Inverted confocal microscope for sample imaging
Fiji	NIH (ImageJ)	open source software (v1.52h)	Image processing package based on ImageJ
Long working distance water immersion objective	Leica	15506360	HC PL APO 40x/1.10 W motCORR CS2
Vibratome	Leica	VT1200S	Sample slicing
Workstation	Dell	Precision 7920	CPU: Intel Xeon Gold 5118 GPU: Nvidia Quadro P5000 RAM: 128 GB 2666 MHz DDR4 SSD: 2 TB
Primary antibodies			
Goat anti-RABV N	Friedrich-Loeffler-Institut		Monospecific polyclonal goat anti-RABV N serum, generated by goat immunization with baculovirus-expressed and His-tag-purified RABV nucleoprotein N Dilution: 1:400
Rabbit anti-GFAP	Dako	Z0334	Polyclonal antibody (RRID:AB_10013382) Dilution: 1:100
Rabbit anti-MAP2	Abcam	ab32454	Polyclonal antibody (RRID:AB_776174) Dilution: 1:250
Rabbit anti-RABV P 160-5	Friedrich-Loeffler-Institut		Monospecific polyclonal rabbit anti-RABV P serum, generated by rabbit immunization with baculovirus-expressed and His-tag-purified RABV phosphoprotein P (see reference 23: Orbanz et al., 2010) Dilution: 1:1,000
Secondary antibodies			

Donkey anti-goat IgG	Thermo Fisher Scientific	depending on conjugated fluorophore	Highly cross-absorbed Dilution: 1:500
Donkey anti-mouse IgG	Thermo Fisher Scientific	depending on conjugated fluorophore	Highly cross-absorbed Dilution: 1:500
Donkey anti-rabbit IgG	Thermo Fisher Scientific	depending on conjugated fluorophore	Highly cross-absorbed Dilution: 1:500
Goat anti-mouse IgG	Thermo Fisher Scientific	depending on conjugated fluorophore	Highly cross-absorbed Dilution: 1:500
Goat anti-rabbit IgG	Thermo Fisher Scientific	depending on conjugated fluorophore	Highly cross-absorbed Dilution: 1:500



1 Alewife Center #200
Cambridge, MA 02140
tel. 617.945.9051
www.jove.com

ARTICLE AND VIDEO LICENSE AGREEMENT

Title of Article:

High-Resolution 3D Imaging of Rabies Virus Infection in Solvent-Cleared Brain Tissue

Author(s):

Luca Zaeck, Madlin Potratz, Conrad M. Freuling, Thomas Müller, Stefan Finke

Item 1 (check one box): The Author elects to have the Materials be made available (as described at <http://www.jove.com/author>) via: ☒ Standard Access ☐ Open Access

Item 2 (check one box):

- ☒ The Author is NOT a United States government employee.
- ☐ The Author is a United States government employee and the Materials were prepared in the course of his or her duties as a United States government employee.
- ☐ The Author is a United States government employee but the Materials were NOT prepared in the course of his or her duties as a United States government employee.

ARTICLE AND VIDEO LICENSE AGREEMENT

1. **Defined Terms.** As used in this Article and Video License Agreement, the following terms shall have the following meanings: "Agreement" means this Article and Video License Agreement; "Article" means the article specified on the last page of this Agreement, including any associated materials such as texts, figures, tables, artwork, abstracts, or summaries contained therein; "Author" means the author who is a signatory to this Agreement; "Collective Work" means a work, such as a periodical issue, anthology or encyclopedia, in which the Materials in their entirety in unmodified form, along with a number of other contributions, constituting separate and independent works in themselves, are assembled into a collective whole; "CRC License" means the Creative Commons Attribution-Non Commercial-No Derivs 3.0 Unported Agreement, the terms and conditions of which can be found at: <http://creativecommons.org/licenses/by-nc-nd/3.0/legalcode>; "Derivative Work" means a work based upon the Materials or upon the Materials and other pre-existing works, such as a translation, musical arrangement, dramatization, fictionalization, motion picture version, sound recording, art reproduction, abridgment, condensation, or any other form in which the Materials may be recast, transformed, or adapted; "Institution" means the institution, listed on the last page of this Agreement, by which the Author was employed at the time of the creation of the Materials; "JoVE" means MyJoVE Corporation, a Massachusetts corporation and the publisher of *The Journal of Visualized Experiments*; "Materials" means the Article and / or the Video; "Parties" means the Author and JoVE; "Video" means any video(s) made by the Author, alone or in conjunction with any other parties, or by JoVE or its affiliates or agents, individually or in collaboration with the Author or any other parties, incorporating all or any portion of the Article, and in which the Author may or may not appear.

2. **Background.** The Author, who is the author of the Article, in order to ensure the dissemination and protection of the Article, desires to have the JoVE publish the Article and create and transmit videos based on the Article. In furtherance of such goals, the Parties desire to memorialize in this Agreement the respective rights of each Party in and to the Article and the Video.

3. **Grant of Rights in Article.** In consideration of JoVE agreeing to publish the Article, the Author hereby grants to JoVE, subject to Sections 4 and 7 below, the exclusive, royalty-free, perpetual (for the full term of copyright in the Article, including any extensions thereto) license (a) to publish, reproduce, distribute, display and store the Article in all forms, formats and media whether now known or hereafter developed (including without limitation in print, digital and electronic form) throughout the world, (b) to translate the Article into other languages, create adaptations, summaries or extracts of the Article or other Derivative Works (including, without limitation, the Video) or Collective Works based on all or any portion of the Article and exercise all of the rights set forth in (a) above in such translations, adaptations, summaries, extracts, Derivative Works or Collective Works and (c) to license others to do any or all of the above. The foregoing rights may be exercised in all media and formats, whether now known or hereafter devised, and include the right to make such modifications as are technically necessary to exercise the rights in other media and formats. If the "Open Access" box has been checked in Item 1 above, JoVE and the Author hereby grant to the public all such rights in the Article as provided in, but subject to all limitations and requirements set forth in, the CRC License.

ARTICLE AND VIDEO LICENSE AGREEMENT

4. **Retention of Rights in Article.** Notwithstanding the exclusive license granted to JoVE in Section 3 above, the Author shall, with respect to the Article, retain the non-exclusive right to use all or part of the Article for the non-commercial purpose of giving lectures, presentations or teaching classes, and to post a copy of the Article on the Institution's website or the Author's personal website, in each case provided that a link to the Article on the JoVE website is provided and notice of JoVE's copyright in the Article is included. All non-copyright intellectual property rights in and to the Article, such as patent rights, shall remain with the Author.

5. **Grant of Rights in Video – Standard Access.** This Section 5 applies if the "Standard Access" box has been checked in Item 1 above or if no box has been checked in Item 1 above. In consideration of JoVE agreeing to produce, display or otherwise assist with the Video, the Author hereby acknowledges and agrees that, Subject to Section 7 below, JoVE is and shall be the sole and exclusive owner of all rights of any nature, including, without limitation, all copyrights, in and to the Video. To the extent that, by law, the Author is deemed, now or at any time in the future, to have any rights of any nature in or to the Video, the Author hereby disclaims all such rights and transfers all such rights to JoVE.

6. **Grant of Rights in Video – Open Access.** This Section 6 applies only if the "Open Access" box has been checked in Item 1 above. In consideration of JoVE agreeing to produce, display or otherwise assist with the Video, the Author hereby grants to JoVE, subject to Section 7 below, the exclusive, royalty-free, perpetual (for the full term of copyright in the Article, including any extensions thereto) license (a) to publish, reproduce, distribute, display and store the Video in all forms, formats and media whether now known or hereafter developed (including without limitation in print, digital and electronic form) throughout the world, (b) to translate the Video into other languages, create adaptations, summaries or extracts of the Video or other Derivative Works or Collective Works based on all or any portion of the Video and exercise all of the rights set forth in (a) above in such translations, adaptations, summaries, extracts, Derivative Works or Collective Works and (c) to license others to do any or all of the above. The foregoing rights may be exercised in all media and formats, whether now known or hereafter devised, and include the right to make such modifications as are technically necessary to exercise the rights in other media and formats. For any Video to which this Section 6 is applicable, JoVE and the Author hereby grant to the public all such rights in the Video as provided in, but subject to all limitations and requirements set forth in, the CRC License.

7. **Government Employees.** If the Author is a United States government employee and the Article was prepared in the course of his or her duties as a United States government employee, as indicated in Item 2 above, and any of the licenses or grants granted by the Author hereunder exceed the scope of the 17 U.S.C. 403, then the rights granted hereunder shall be limited to the maximum rights permitted under such

statute. In such case, all provisions contained herein that are not in conflict with such statute shall remain in full force and effect, and all provisions contained herein that do so conflict shall be deemed to be amended so as to provide to JoVE the maximum rights permissible within such statute.

8. **Likeness, Privacy, Personality.** The Author hereby grants JoVE the right to use the Author's name, voice, likeness, picture, photograph, image, biography and performance in any way, commercial or otherwise, in connection with the Materials and the sale, promotion and distribution thereof. The Author hereby waives any and all rights he or she may have, relating to his or her appearance in the Video or otherwise relating to the Materials, under all applicable privacy, likeness, personality or similar laws.

9. **Author Warranties.** The Author represents and warrants that the Article is original, that it has not been published, that the copyright interest is owned by the Author (or, if more than one author is listed at the beginning of this Agreement, by such authors collectively) and has not been assigned, licensed, or otherwise transferred to any other party. The Author represents and warrants that the author(s) listed at the top of this Agreement are the only authors of the Materials. If more than one author is listed at the top of this Agreement and if any such author has not entered into a separate Article and Video License Agreement with JoVE relating to the Materials, the Author represents and warrants that the Author has been authorized by each of the other such authors to execute this Agreement on his or her behalf and to bind him or her with respect to the terms of this Agreement as if each of them had been a party hereto as an Author. The Author warrants that the use, reproduction, distribution, public or private performance or display, and/or modification of all or any portion of the Materials does not and will not violate, infringe and/or misappropriate the patent, trademark, intellectual property or other rights of any third party. The Author represents and warrants that it has and will continue to comply with all government, institutional and other regulations, including, without limitation all institutional, laboratory, hospital, ethical, human and animal treatment, privacy, and all other rules, regulations, laws, procedures or guidelines, applicable to the Materials, and that all research involving human and animal subjects has been approved by the Author's relevant institutional review board.

10. **JoVE Discretion.** If the Author requests the assistance of JoVE in producing the Video in the Author's facility, the Author shall ensure that the presence of JoVE employees, agents or independent contractors is in accordance with the relevant regulations of the Author's institution. If more than one author is listed at the beginning of this Agreement, JoVE may, in its sole discretion, elect not take any action with respect to the Article until such time as it has received complete, executed Article and Video License Agreements from each such author. JoVE reserves the right, in its absolute and sole discretion and without giving any reason therefore, to accept or decline any work submitted to JoVE. JoVE and its employees, agents and independent contractors shall have

ARTICLE AND VIDEO LICENSE AGREEMENT

full, unfettered access to the facilities of the Author or of the Author's institution as necessary to make the Video, whether actually published or not. JoVE has sole discretion as to the method of making and publishing the Materials, including, without limitation, to all decisions regarding editing, lighting, filming, timing of publication, if any, length, quality, content and the like.

11. **Indemnification.** The Author agrees to indemnify JoVE and/or its successors and assigns from and against any and all claims, costs, and expenses, including attorney's fees, arising out of any breach of any warranty or other representations contained herein. The Author further agrees to indemnify and hold harmless JoVE from and against any and all claims, costs, and expenses, including attorney's fees, resulting from the breach by the Author of any representation or warranty contained herein or from allegations or instances of violation of intellectual property rights, damage to the Author's or the Author's institution's facilities, fraud, libel, defamation, research, equipment, experiments, property damage, personal injury, violations of institutional, laboratory, hospital, ethical, human and animal treatment, privacy or other rules, regulations, laws, procedures or guidelines, liabilities and other losses or damages related in any way to the submission of work to JoVE, making of videos by JoVE, or publication in JoVE or elsewhere by JoVE. The Author shall be responsible for, and shall hold JoVE harmless from, damages caused by lack of sterilization, lack of cleanliness or by contamination due to the making of a video by JoVE its employees, agents or independent contractors. All sterilization, cleanliness or decontamination procedures shall be solely the responsibility of the Author and shall be undertaken at the Author's

expense. All indemnifications provided herein shall include JoVE's attorney's fees and costs related to said losses or damages. Such indemnification and holding harmless shall include such losses or damages incurred by, or in connection with, acts or omissions of JoVE, its employees, agents or independent contractors.

12. **Fees.** To cover the cost incurred for publication, JoVE must receive payment before production and publication the Materials. Payment is due in 21 days of invoice. Should the Materials not be published due to an editorial or production decision, these funds will be returned to the Author. Withdrawal by the Author of any submitted Materials after final peer review approval will result in a US\$1,200 fee to cover pre-production expenses incurred by JoVE. If payment is not received by the completion of filming, production and publication of the Materials will be suspended until payment is received.

13. **Transfer, Governing Law.** This Agreement may be assigned by JoVE and shall inure to the benefits of any of JoVE's successors and assignees. This Agreement shall be governed and construed by the internal laws of the Commonwealth of Massachusetts without giving effect to any conflict of law provision thereunder. This Agreement may be executed in counterparts, each of which shall be deemed an original, but all of which together shall be deemed to be one and the same agreement. A signed copy of this Agreement delivered by facsimile, e-mail or other means of electronic transmission shall be deemed to have the same legal effect as delivery of an original signed copy of this Agreement.

A signed copy of this document must be sent with all new submissions. Only one Agreement required per submission.

CORRESPONDING AUTHOR:

Name:
Department:
Institution:
Article Title:
Signature: Date:

Please submit a signed and dated copy of this license by one of the following three methods:

- 1) Upload a scanned copy of the document as a pdf on the JoVE submission site;
- 2) Fax the document to +1.866.381.2236;
- 3) Mail the document to JoVE / Attn: JoVE Editorial / 1 Alewife Center #200 / Cambridge, MA 02139

For questions, please email submissions@jove.com or call +1.617.945.9051

Line numbers refer to the revised manuscript. For improved intelligibility, line numbers have also been added to the editorial comments from the manuscript, which are included at the end of this rebuttal document. When referencing specific sections of the manuscript, an underscore highlights edits.

Editorial comments:

“1. The editor has formatted the manuscript to match the journal's style. Please retain the same.”

To also retain coherency, order of paragraphs or sentences has been adjusted where needed (refer to the first two comments from the manuscript shown below). The overall format established by the editor has been retained.

“2. Please address all the specific comments marked in the manuscript.”

All comments in the manuscript have been addressed. The comments have been answered in the manuscript and, for improved intelligibility, are also included in this rebuttal document.

“3. Once done please ensure that the highlight is no more than 2.75 pages including headings and spacings.”

The highlight for scripting and filming has been reviewed and is about 2.75 pages long.

Editorial comments from the manuscript:

“We cannot have paragraphs of text in the protocol section (referring to lines 104ff.). Hence moved here.

Protocol should only be made of discrete steps showing actions.”

Instead of moving the section about precautions when handling rabies virus to the end of the introduction, where it does not really fit into, we have now combined it with the already existing precautionary paragraph about the chemical hazards of the protocol. This also eliminates the additional paragraph but retains more coherency.

“Combined the background and note as we cannot have paragraph of text in the protocol section (lines 127ff., 164ff., 206ff., and 220ff.).”

We changed the order of the combined paragraph (note first, background second) in all cases to improve coherency and intelligibility.

“Please refer to the supplementary file (lines 257ff.) as well and include it in the figure legend.”

We have now added a reference to the 3D printing file (.STL file) that can be found in the supplement of this publication. A reference was already included in the figure legend of the corresponding Figure 2.

lines 257ff. (6.1.): Using a 3D printer, print imaging chamber and lid (material: Copolyester [CPE], nozzle: 0.25 mm, layer height: 0.06 mm, wall thickness: 0.88 mm, wall count: 4, infill: 100%, no support structure; the corresponding .STL file can be found in the supplementary materials of this protocol).

“Please expand (BABB-D15) during first time use.”

The abbreviation has been defined on first use (line 239f.).

“For this section, please provide all the graphical user interface, button clicks, knob turns etc. to show how is a step performed.”

We have now added an exemplary workflow of how to process large image stacks to generate 3D projections using ImageJ (7.3.x.).

However, we did not add any further detail explanation for the image acquisition part (7.1. and 7.2.). Potential users will most likely be using a variety of microscopy set-ups from different manufacturers and varying types of acquisition software. We have specified the type of microscope and objective we used in the Table of Materials that is attached to this publication. Together with the values and parameters we already provided here (7.1.1. and 7.2.1.), we are confident that each microscope user can input these settings into their individual microscopy systems. Further explanation and detailed descriptions would only benefit users with the very same microscope and, thus, in our opinion only clutter the protocol.

“Please provide reprint permission for this figure.”

The figure legend for Figure 1A has been poorly phrased. The graphical representation of the workflow has not been taken from either publication but has in fact been made by us and is based on written text from the two publications already mentioned in the figure legend. We, thus, have rephrased the figure legend to avoid ambiguity.

lines 364f.: (A) Graphical representation of the workflow based on the protocols from Renier et al. (2014)¹⁴ and Pan et al. (2016)¹³.

“Please provide a scale bar for all the microscopic images for example RABVP and TO_PRO3 etc.”

It is common practice in depiction of immunofluorescence images to provide scale bars for the merge images only. This aims to declutter the overall image composition and improve comprehensibility. In all non-3D images included in this publication, a scale bar is included in the merge image. As the relative scale in the single channel images, albeit usually being depicted smaller in size, is the very same as in the respective merge image, distances and lengths can still easily be estimated. Therefore, for the reasons mentioned above, we would prefer not to include any additional scale bars in those images, if not necessary.

“The panel C is not marked in the figure.”

The two lower panels in Figure 6 have now been marked as Figure 6C (bottom left) and Figure 6D (bottom right) for improved referencing and intelligibility of the figure.



Click here to access/download
Supplemental Coding Files
3D_ImagingChamber.stl